# Lithium-ion Batteries Aging Motinoring Througth Open Circuit Voltage (OCV) Curve Modelling and Adjustment

Loic Lavigne[1], Jocelyn Sabatier[1], Junior Mbala Francisco[2],
Franck Guillemard[2] and Agneiszka Noury[2]

*[1]IMS Laboratory, UMR 5218 CNRS, Bordeaux University, 351 Cours de la Libération, 33405 Talence, France*
*[2]PSA Peugeot Citroën ,2 Route de Gisy, 78943 Vélizy-Villacoublay, France*

Keywords: Lithium-ion Cell, Open Circuit Voltage (OCV) Curve Adjustment, Battery Aging Monitoring.

Abstract: This paper is a contribution to lithium-ion batteries modeling tacking into account aging effects. It first analyses the impact of aging on electrode stoichiometry and then on lithium-ion cell Open Circuit Voltage (OCV) curve. Through some hypotheses and an appropriate definition of the cell state of charge, it shows that each electrode equilibrium potential, but also the whole cell equilibrium potential can be modelled by a polynomial that requires only one adjustment parameter during aging. An adjustment algorithm, based on the idea that for two fixed OCVs, the state of charge between these two equilibrium states is unique for a given aging level, is then proposed. Its efficiency is evaluated on a battery pack constituted of four cells. This adjustment parameter can thus be viewed as a State Of Health (SOH) or aging indicator.

## 1 INTRODUCTION

Due to their high energy and power densities compared to other existing technologies, Li-ion batteries are increasingly used as energy storage system in mobile applications (Armand and Tarascon, 2008). The onboard Li-ion battery packs have to work together with reliable battery management systems (BMS) to ensure their optimal and safe use (Liaw et al, 2010). Among the tasks ensured by the BMS, State-Of-Charge (SOC) estimation is of an extreme importance. The energy management strategies in hybrid vehicles, for instance, rely on the accurate knowledge of the SOC, the latter being an indicator of available energy. SOC estimation methods commonly used impose a characterization of the Open Circuit Voltage (OCV) curve (through a polynomial, a look-up table, …) as they use :

- either a direct OCV curve inversion methods (if the application permits cells steady state voltage measurement) (Lee et al, 2008),
- or cells models based methods (Plett, 2004), (Kim, 2010), (Sabatier et al, 2014), (Francisco et al, 2014), (Sabatier et al, 2015).

As OCV is closely related to SOC, the SOC

estimators require an accurate OCV model (Piller et al, 2001), (Santhanagopalan and White, 2006).

However, at battery aging, the OCV curve of each cell changes as OCV reflect battery aging and performance degradation (Roscher et al, 2011). The impact of aging on cell equilibrium voltage is analyzed in (Schmidt and al, 2013). This change distorts the estimator if nothing is done to adjust the curve law. Aging correction can be thus implemented as done in (Cheng et al, 2015). But this class of methods does not take into account the underlying physical phenomenon of lithium-ion intercalation process. This knowledge makes possible analytical descriptions of the OCV curve and then permits the implementation of accurate estimation methods for both SOC and State of Health (SOH). Some of these methods are known in the literature as incremental capacity analysis (ICA) technique (Dubarry and Liaw, 2009) or the differential voltage analysis (DVA) (Honkuraa et al, 2008).

Most of the analytical descriptions for OCV curve available in the literature involve a large number of parameter (Hu et al, 2011), (Weng et al, 2014) that all must be adjusted as battery aging. This imposes to implement complex and resources consuming on-board iterative optimization

algorithms.

In this paper, a new polynomial parametrization for OCV curve is proposed. As ageing of lithium-ion cell, only one parameter must be adjusted to ensure an accurate fitting of the OCV curve by the polynomial. Such a parametrization results in an analysis of the cell using "communicating vessels" idea introduced in (Schmidt and al, 2013). If each electrode equilibrium voltages at the unused state is modelled as in (Karthikeyan et al, 2008), introduction of some simplifying hypothesis permits to show that the OCV curve can be modelled by a polynomial that requires only one adjustment parameter during aging. An adjustment algorithm, based on the idea that for two fixed OCVs, the state of charge between these two equilibrium state is unique for a given aging level, is then proposed. Its efficiency is evaluated on a battery pack constituted of four cells.

## 2 PARAMETRIZATION OF A LITHIUM-ION CELL OCV

### 2.1 Notations and Electrode Equilibrium Potential Definition

It is supposed in the sequel that subscript $p$ and $n$ are used to denote respectively the positive and the negative electrode of a lithium-ion cell. Electrodes stoichiometry $x_i$, $i \in \{p, n\}$ (Bard et al., 2008) are defined as the ratio of the inserted lithium quantities $Q_i$ over the maximal theoretical quantities that can be inserted $Q_{i,max}$:

$$x_i(t) = \frac{Q_i(t)}{Q_{i,\max}(t)} \tag{1}$$

If $T$ denotes the temperature, cell OCV can be defined using the equilibrium potentials of the two electrodes, by:

$$E(T) = E_p(x_p, T) - E_n(x_n, T), \tag{2}$$

positive electrode equilibrium potential, denoted $E_p(x_p, T)$, and negative electrode equilibrium potential, denoted $E_n(x_n, T)$, being respectively defined by:

$$E_i(x_i, T) = V_{Nernst}(x_i, T) + V_{INT}(x_i) \\ i \in \{n, p\} \tag{3}$$

Using standard potential $E_i^0$, Nernst potential $V_{Nernst}(x_i, T)$, is defined by the relation

$$V_{Nernst}(x_i, T) = E_i^0 + \frac{RT}{F} \ln\left(\frac{1-x_i}{x_i}\right) \\ i \in \{n, p\}. \tag{4}$$

In the previous relation, $R$ denotes the universal gas constant ($R = 8.314\,472$ J K$^{-1}$ mol$^{-1}$) and $F$ is the Faraday constant ($F=96485.33$°C mol$^{-1}$). Among the models available in the literature for $V_{INT}(x_i)$, Redlich-Kister model given by the following relation is used in the sequel (Karthikeyan, Sikha, and White 2008) with $i \in \{n, p\}$:

$$V_{INT}(x_i) = \sum_{k=0}^{K_i} A_{i,k} \left[ (2x_i - 1)^{k+1} - \frac{2x_i k (1-x_i)}{(2x_i - 1)^{1-k}} \right] \tag{5}$$

It is the expression of $V_{INT}$ (for non-ideal interaction), that gives the closest experimental measures fitting as shown in Figure 1, comparing to several other equilibrium potential laws (Karthikeyan, Sikha, and White 2008).

**Remark 1 -** According to relation (21) and (22) in (Karthikeyan, Sikha, and White 2008), note that a linear dependence to temperature can be introduced in coefficients $A_{i,k}$ to take into account temperature variations: $A_{i,k}(T) = a_{i,k}T$ ($a_{i,k}$ being an additional parameter for temperature dependence such as for $A_{i,k} = a_{i,k}T_0$ for parameters $A_{i,k}$ in relation (5) and for a reference temperature $T_0$).
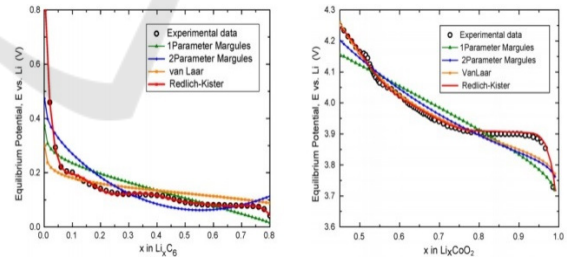


Figure 1: Comparison of various equilibrium electrode potentials laws for experimental data fitting (Karthikeyan, Sikha, and White 2008).

### 2.2 Polynomial Approximations of Electrode Equilibrium Potentials

The goal now is to make simplifying assumptions in order to obtain polynomial expressions for electrodes equilibrium potentials.

Given that

$$\ln\left(\frac{1-x_i}{x_i}\right) = \ln(1-x_i) - \ln(1+(x_i-1)) \qquad (6)$$

$$i \in \{n, p\}$$

expansion of $\ln((1-x)/x)$ on $x \in \left]0, 1\right[$ is given by:

$$\ln\left(\frac{1-x_i}{x_i}\right) = -\sum_{k=0}^{\infty}\frac{x_i^{k+1}}{k+1} - \sum_{k=0}^{\infty}(-1)^{k+1}\frac{(x_i-1)^{k+1}}{k+1} \quad (7)$$

with $i \in \{n, p\}$ and permits the following approximation, denoted $\widetilde{V}_{Nernst}(x_i, T)$, for relation (4):

$$V_{Nernst}(x_i, T) \approx E_i^0$$
$$+ \frac{RT}{F}\sum_{k=0}^{N_{LN}^i}\frac{1}{k+1}\left[(-1)^{k+1}(x_i-1)^{k+1} - x_i^{k+1}\right] \qquad (8)$$

Thus, for a large enough $N_{LN}^i$, the function $RT\ln((1-x_i)/x_i)/F$ can be reduced to a polynomial. By way of illustration, Figure 2 shows that the approximation error $V_{Nernst}(x_i, T) - \widetilde{V}_{Nernst}(x_i, T)$ remains minor and limited to a few millivolts and also shows a low impact of temperature $T$.

Thus, using relation (8) and through expansion of relation (5), electrode equilibrium potentials in relation (2) can be written in polynomial form:

$$E_i = \sum_{k=0}^{N_i}\overline{A_{i,k}}(x_i)^k \qquad\qquad (9)$$
$$i \in \{n, p\}$$

with

$$N_i = \max\left(K_i; N_{LN}^i\right). \qquad (10)$$

where coefficients $\overline{A_{i,k}}$ are combinations of coefficients $A_{i,k}$ of relation (5).

As shown in the application section, temperature has a low impact on coefficients $\overline{A_{i,k}}$ but according to remark 1, temperature dependence can be introduced in coefficients $\overline{A_{i,k}}$ and thus relation (9) can be rewritten as:

$$E_i = \overline{a_i^0} + \overline{a_i^1}T + \sum_{k=1}^{N_i}\overline{a_{i,k}}T(x_i)^k \qquad i \in \{n, p\}. \quad (11)$$

## 2.3 Ageing Effects on Electrodes Stoichiometry

From relation (9), cell OCV depends on:
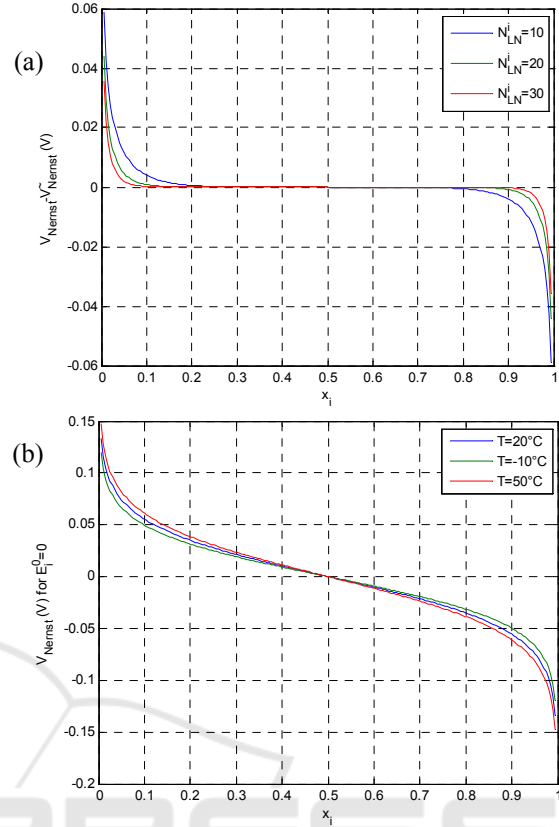


Figure 2: Approximation error between $V_{Nernst}(x_i, T) - \widetilde{V}_{Nernst}(x_i, T)$ for various values of $N^i{}_{LN}$ (a) and impact of the temperature on $V_{Nernst}(x_i, T)$ with $E_i^0 = 0$ (b).

- parameters $E_i^0$, $A_{i,k}$ and more weakly on the temperature T;

- electrodes stoichiometries $x_i$ which themselves depends on the amount of inserted lithium $Q_i$ and the maximal theoretical capacity $Q_{i,\max}$ according to relation (1).

In agreement with the authors of (Karthikeyan et al. 2008), the following assumption is made on coefficients $A_{i,k}$.

### Hypothesis 1
*For a constant temperature, coefficients $A_{i,k}$ of Redlich-Kister model are supposed constants as intrinsic to the electrode electrochemistry* ∎

As a consequence, coefficients $A_{i,k}$ are not affected by the cell aging. Aging is then necessarily passed on electrodes stoichiometry $x_p$ and $x_n$.

Specifically, it is then expected that the only aging reactions impacting the cell OCV are those resulting in at least one of the following effects:

- a change in the electrode geometry, (eg formation of dendritic deposits (Arora et al. 1998)) this change impacting the cell theoretical maximum capacity $Q_{i,\max}$ and thus the stoichiometry $x_i(t)$ linked to the amount of charge $Q_i(t)$ in electrode $i$;

- a loss $Li^+$ cycling ions (ion consumption in aging reactions).

Since the cell OCV characterizes a cell at rest, charge transfer equations can be ignored in the following developments. For the analysis of $Li^+$ cycling ions concentration, the cell will be represented by two communicating tanks as in (Po et al. 2007).

In the previous equations, the OCV is expressed according to electrode stoichiometries. We now establish the link between the electrode stoichiometries and the SOC (estimated in practice). This last one is defined by the relation:

$$SOC = \frac{Q_{dispo}}{Q_{ref}} \qquad (12)$$

where $Q_{dispo}$ is the possible capacity extractible of the cell. In usual definition of SOC, $Q_{ref}$ is the cell maximum capacity which varies with aging cells. This is a problem if OCV adjustment during aging requires SOC measures, as SOC definition requires the cell real capacity knowledge which is precisely to identify. To treat this problem, the $Q_{ref}$ uncertainty during aging is eliminated by adopting the following definition:

**Definition 1**

$$SOC(t) = \begin{vmatrix} 100\% \ if \ E = E_{100\%} \\ 0 \ if \ \int\limits_{E_{100\%}}^{E(t)} I = Q_{ref} (= Cons \tan t) \end{vmatrix} \qquad (13)$$

■
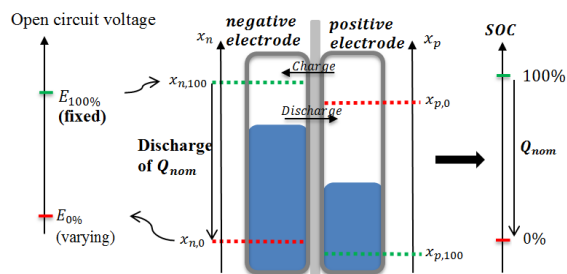


Figure 3: Link between the electrodes stoichiometry and the SOC.

This definition imposes

- a SOC equal to 100% when OCV is maximum and equal to $E_{100\%}$ (for example 4V) for all cells ageing.

- a SOC equal to 0% after discharge, starting to $E = E_{100\%}$, and a fixed $Q_{ref}$. The $Q_{ref}$ choice is not important and is determined by the user. In practice the reference capacity is usually fixed to the nominal capacity ($Q_{ref} = Q_{nom}$). Definition 1 is illustrated in Figure 3.

For an electrode $i$ ($i \in \{n, p\}$), and as illustrated by Figure 4, the available capacity can be defined by:

$$Q_{av} = Q_i - Q_{i,0} \qquad (14)$$

where $Q_{i,0}$ is the capacity in the electrode at $SOC = 0$, then $x_{i,0} = Q_{i,0}/Q_{i,\max}$ is the electrode stoichiometry for $SOC = 0\%$.
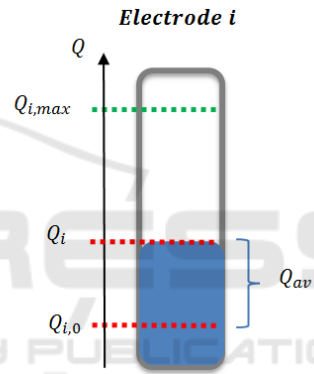


Figure 4: Available capacity definition for an electrode.

From relation (1) and previous analysis:

$$x_i(t) = \frac{Q_i(t)}{Q_{i,\max}(t)} - \underbrace{\frac{Q_{i,0}(t)}{Q_{i,\max}(t)} + x_{i,0}}_{=0} \qquad (15)$$

then

$$x_i(t) = \frac{Q_i(t) - Q_{i,0}(t)}{Q_{i,\max}(t)} + x_{i,0} = \frac{Q_{dispo}(t)}{Q_{i,\max}(t)} + x_{i,0} \qquad (16)$$

or

$$x_i(t) = \frac{Q_{ref}(t)Q_{dispo}(t)}{Q_{i,\max}(t)Q_{ref}(t)} + x_{i,0} \qquad (17)$$

and finally

$$x_i(t) = \frac{Q_{ref}(t)}{Q_{i,\max}(t)} SOC(t) + x_{i,0} \qquad (18)$$

Then, for $SOC = 100\%$, the following equation is

verified $x_{i,100}(t) - x_{i,0}(t) = Q_{ref}(t)/Q_{i,\max}(t)$.

The previous analysis shows that the electrode stoichiometries are proportional to the *SOC* and can be written:

$$x_p(t) = (x_{p,100} - x_{p,0})SOC + x_{p,0}$$
$$x_n(t) = (x_{n,100} - x_{n,0})SOC + x_{n,0} \tag{19}$$

Let us consider a given state of charge *SOC*. The corresponding OCV is varying with cell aging, excepted for the point *SOC* =100% (according to definition 1). For the positive electrode, this change modifies the parameter $x_{p,0}$ which is then depending of cell aging ($x_{p,0} \Rightarrow x_{p,0}(age)$). The parameter $\alpha_p(age)$ is then introduced such as:

$$x_p(t) = \frac{-Q_{ref}}{Q_{p,\max}^{init}} \alpha_p(age)SOC(t) + x_{p,0}(age) \tag{20}$$

or with a more compact form :

$$x_p(t) = \overline{\alpha}_p(age)SOC(t) + \overline{\beta}_p(age), \tag{21}$$

where

$$\overline{\alpha}_p(age) = \frac{-Q_{ref}}{Q_{p,\max}^{init}} \alpha_p(age)$$
$$\overline{\beta}_p(age) = x_{p,0}(age) \tag{22}$$

The same equation holds for the negative electrode with parameters $\overline{\alpha}_n(age)$ and $\overline{\beta}_n(age)$:

$$x_n(t) = \overline{\alpha}_n(age)SOC(t) + \overline{\beta}_n(age) \tag{23}$$

## 2.4 Open Circuit Voltage Parametrization with Knowledges of Each Cell Equilibrium Potential

In this section, equilibrium potentials $E_p$ and $E_n$, and then coefficients $\overline{A_{p,k}}$ and $\overline{A_{n,k}}$ are supposed known. From relations (21) and (23), the equilibrium potentials $E_p$ and $E_n$ given by relation (9) can be expressed as a function of cell ageing with the 4 parameters $\overline{\alpha}_p(age)$, $\overline{\beta}_p(age)$, $\overline{\alpha}_n(age)$ and $\overline{\beta}_n(age)$, and thus relation (2) becomes:

$$E = \sum_{k=0}^{N_p} \overline{A_{p,k}} \left( \overline{\alpha}_p(age)SOC + \overline{\beta}_p(age) \right)^k$$
$$- \sum_{k=0}^{N_n} \overline{A_{n,k}} \left( \overline{\alpha}_n(age)SOC + \overline{\beta}_n(age) \right)^k \tag{24}$$

The OCV adjustment problem after ageing consists in the identification of these 4 parameters.

This adjustment can for instance, be realized with a set of *M* measures $\left\{ SOC_j ; E_j \right\}_{j \in [1;M]}$ through minimization of criteria:

$$J = \frac{1}{M} \sum_{j=1}^{M} \left[ \begin{array}{c} E_J - E_p\left( \overline{\alpha}_p(age)SOC + \overline{\beta}_p(age) \right) \\ + E_n\left( \overline{\alpha}_n(age)SOC + \overline{\beta}_n(age) \right) \end{array} \right]^2, \tag{25}$$

with the constraint:

$$\mathcal{C} : E_{100\%} = \sum_{k=0}^{N_p} \overline{A_{p,k}} \left( \overline{\alpha}_p(age) + \overline{\beta}_p(age) \right)^k$$
$$- \sum_{k=0}^{N_n} \overline{A_{n,k}} \left( \overline{\alpha}_n(age) + \overline{\beta}_n(age) \right)^k \tag{26}$$

As the *SOC* definition given by relation (13) imposes a fixed $Q_{ref}$ capacity, estimation of $\left( \overline{\alpha}_p ; \overline{\alpha}_n \right)$ supplies maximum capacities estimations $Q_{p,\max}$ and $Q_{n,\max}$.

## 2.5 Open Circuit Voltage Parametrization without Knowledge of Each Cell Equilibrium Potential

When equilibrium potentials $E_p$ and $E_n$ are not known (practical case), $\overline{A_{p,k}}$ and $\overline{A_{n,k}}$ coefficients become unknowns. The only OCV curve available is an experimental measure of this one obtained from the interpolation of a set of OCV measures with large *SOC* variations. This OCV curve will be noted *OCVC_{init}*. A study of different OCV measure technics is given in (Petzl and Danzer, 2013).

Measures in charge and discharge are used to determine the OCV curve. An average curve obtained with a charge curve and a discharge curve seems to be the best compromise because of hysteresis effects (Roscher et al. 2011). OCV curves (*OCVC_{init}*) used in the following are determined for discharge measures (see Figure 5).
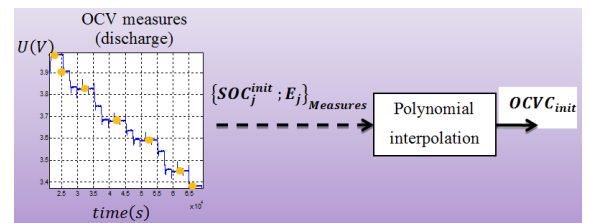


Figure 5: OCVCinit identification with OCV measures.

The curve *OCVC_{init}* obtained with polynomial

interpolation at start time, has the following structure:

$$E_{init} = \sum_{k=0}^{N} D_k^{init} SOC^k \qquad (27)$$

To prove that aging impact on OCV can be expressed like in relation (24), the link between the two electrodes stoichiometries $x_p$ and $x_n$ is now established.

In (Pop et al. 2007), a cell is represented for two communicating tanks according to figure 6.
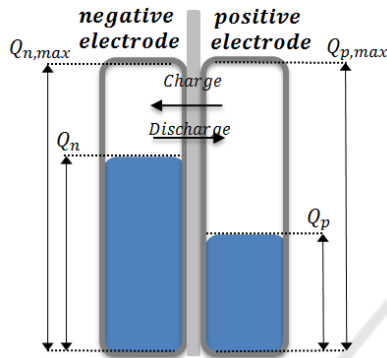


Figure 6: Cell Li-ion simplified scheme.

Figure 6 permits to write the following equation:

$$Q_p + Q_n = Cst \qquad (28)$$

where by dividing by $Q_{p,\max}$:

$$\frac{Q_p}{Q_{p,\max}} + \frac{Q_n}{Q_{p,\max}} = Cst' \qquad (29)$$

and thus

$$x_p + \frac{Q_n}{Q_{n,\max}} \frac{Q_{n,\max}}{Q_{p,\max}} = x_p + \frac{Q_{n,\max}}{Q_{p,\max}} x_n = Cst' \qquad (30)$$

Relation (30) shows that a linear equation can connect the electrode stoichiometries $x_p$ and $x_n$ as:

$$x_p = c_p x_n + d_p \qquad (31)$$

or

$$x_n = c_n x_p + d_n \qquad (32)$$

Then relation (2) becomes:

$$E = \sum_{k=0}^{N_p} \overline{A_{p,k}} (x_p)^k - \sum_{k=0}^{N_n} \overline{A_{n,k}} (c_n x_p + d_n)^k \qquad (33)$$

Expansion of terms in the second sum permits a new relation:

$$E = \sum_{k=0}^{\max\{N_p, N_n\}} D_k (x_p)^k = \sum_{k=0}^{N} D_k (x_p)^k \qquad (34)$$

Coefficients $D_k$ are combinations of coefficients $\overline{A_{p,k}}$, $\overline{A_{n,k}}$, $c_n$ and $d_n$. The ageing impact on the OCV, can then be introduced by relation (21), thus leading to:

$$E = \sum_{k=0}^{N} D_k (\overline{\alpha}_p(age) SOC(t) + \overline{\beta}_p(age))^k \qquad (35)$$

**Remark 2** - According to relation (11) in relation (33), temperature dependence can be introduced in relation (35), leading to

$$E = d^0 + d^1 T + \sum_{k=1}^{N} T d_k (\overline{\alpha}_p(age) SOC(t) + \overline{\beta}_p(age))^k \qquad (36)$$

From relation (35), the OCV adjustment problem after ageing consists in the identification of only the two parameters $\overline{\alpha}_p$ and $\overline{\beta}_p$. This identification can, for instance, be realized with a set of $M$ measures $\{SOC_j; E_j\}_{j \in [1;M]}$ through minimization of criterion:

$$J = \frac{1}{M} \sum_{j=1}^{M} \left[ E_j - E(\overline{\alpha}_p(age) SOC + \overline{\beta}_p(age)) \right]^2 \qquad (37)$$

with constraint:

$$\mathcal{C} : E_{100\%} = \sum_{k=0}^{N} D_k (\overline{\alpha}_p(age) + \overline{\beta}_p(age))^k \qquad (38)$$

## 2.6 Experimental Validation

To experimentally validate the relation (35), several OCV curves stemming from accelerated aging process (described in section 3.1) are now identified by assuming that the *OCV* after aging is given by:

$$E = \sum_{k=0}^{N} D_k (\alpha(age) SOC + \beta(age))^k \qquad (39)$$

Search for $\alpha$ and $\beta$ parameters is performed manually. A wide range of values for $\alpha$ and β are used. For each pair ($\alpha$, $\beta$), the following criterion is evaluated:

$$J_{test}\begin{pmatrix}\alpha\\\beta\end{pmatrix} = \sum_{j=1}^{3}\begin{pmatrix}E_{mesures,j}\\-E\left(\alpha,\beta,D_k,SOC_{mesures,j}\right)\end{pmatrix}^2 . \qquad (40)$$

The three couples of measures $\left(SOC_{mesures,j};E_{mesures,j}\right)$ are derived from a charge profile such as that shown in Figure 7. The pair ($\alpha$, $\beta$) selected minimizes $J_{test}$.
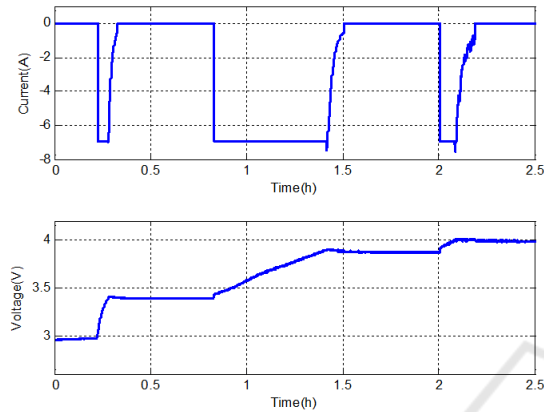


Figure 7: Charge profile example used to get the necessary measures for the OCV curve adjustment.

To validate the pair ($\alpha$, $\beta$) selected, the identified *OCV* curve is compared with the measured *OCV* curve in Figure 8. This figure shows the feasibility of the parametrization given by relation (39) and also shows that the proposed optimization leads to a reliable reconstruction of the *OCV* curve over a wide range of SOC and with a reduced number of voltage measurements (namely three during on a charge profile). Figure 9 shows the shape of the logarithm of $J_{test}$ criterion that exhibits a global minimum.



Initial OCV curve (time $t_0$) for $D_k$ coefficients identification
Aged OCV curve (time $t_0$+3years+ 3 months)
Measures at time $t_0$+3years+ 3 months
Measures for ($\alpha$; $\beta$) identification
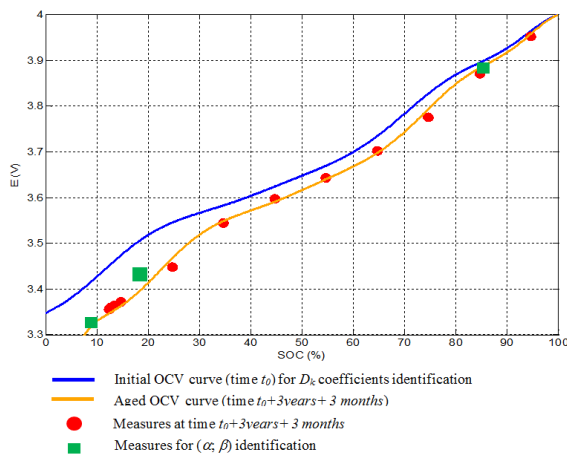
Figure 8: Identification of the OCV curve using charge profile measures and manual search of parameters $\alpha$ and $\beta$ of a cell after two years calendar ageing.

The previous adjustment was performed for several cell aging. From optimal identified pairs ($\alpha$, $\beta$), figure 10 shows the variations of $\beta$ as a function of $\alpha$. This figure shows that parameters $\alpha$ and $\beta$ are linked by the equation $\beta = -\alpha + 1$ which makes it possible to write the relation:

$$SOC_{init} \approx \alpha(SOC-1)+1 \qquad (41)$$

This remark permits to transform the OCV curve adjustment problem after aging to the research for a single parameter: parameter $\alpha$.
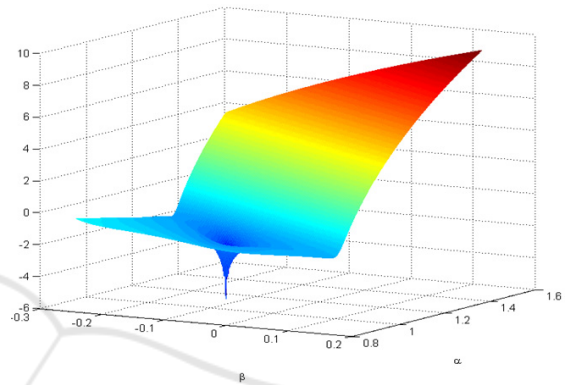


Figure 9: Criterion $J_{test}$ as a function of the pair ($\alpha$; $\beta$).
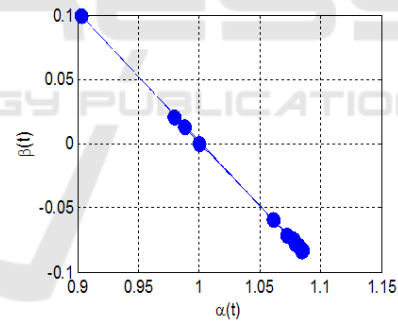


Figure 10: Variation of $\beta$ as a function of $\alpha$.

## 2.7 Unicity of Coefficient $\alpha$ for Each OCV Curve

Coefficient $\alpha$ characterizes the cell capacity loss and is unique for each OCV curve. It is therefore an aging indicator. The uniqueness of $\alpha$ is due to three reasons:

1 - Polynomials defined by coefficients $D_k^{init}$ (relation (27)) is strictly increasing.

2 - $T: SOC \mapsto \alpha(SOC-1)+1$ is an application strictly increasing and that defines a straight line whose slope is $\alpha$.

3 - Equation $E(SOC_1) = E(SOC_2)$ has an unique solution $SOC_1 = SOC_2 = 1$.

Thus

– $\alpha = 1$ corresponds to the initial ageing state;

– $\alpha > 1$ indicates a cell capacity loss. The cell may be considered to be aged.

# 3 OCV MODEL ADJUSTMENT AS AGING

The proposed method has two steps illustrated in figure 11. The first step is the identification of the OCV curve at initial state (using relation (26) thus leading to coefficients $D_k^{init}$ ). In the second step, $\alpha$ parameter characterizing the aging of the cell is identified from at least two OCV measures in normal operation or in specific operation (charge phase for instance).
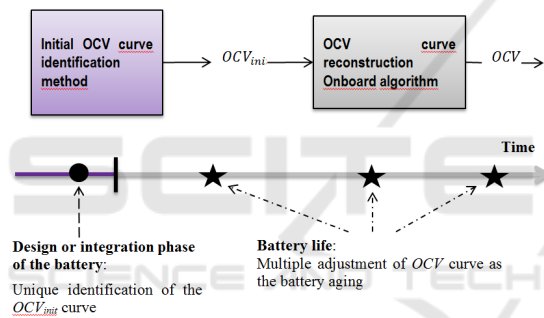


Figure 11: Block diagram of the OCV curve reconstruction method during cell aging.
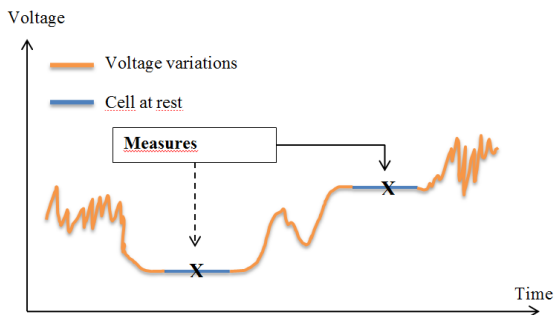


Figure 12: Description of measures and rest periods required for the step two adjustments method implementation.

To implement step 2 of figure 11 method, it is require as shown in figure 12 to have two consecutive rest periods that permits to measure the cell OCV without the cell age has changed significantly between the two measures.

## 3.1 Aging Characterization and Bench Description

The strategy previously described is now applied to a battery pack constituted of four 7 A.h VL6P type lithium-ion cells from JCS-SAFT (LiNiCoAl Oxide). The cells, numbered form 1 to 4, have undergone an accelerated calendar aging at 60°C. The aging phases are punctuated by characterization tests. Characterization tests on Digatron bench include measures of capacity, internal resistance and OCV for each cell and for various temperatures. The chronology of the aging and characterization tests is given in Figure 13.
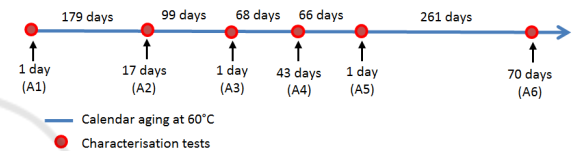


Figure 13: Chronology of calendar aging and characterization tests.

## 3.2 Initial OCV Identification

Each battery cell initial OCV curve $OCVC_{init}$ must be fitted by relation (27) before battery usage. This necessary initial fitting can be time and resource consuming but can be done off-line and is only once realized.

However this relative complexity can be reduced. Hypothesis 1 supposes that coefficients $A_{i,k}$ depend only on electrode electrochemistry and are constant. Then, if the battery is made of the same cells, the same initial OCV curve fitting should be used for all the battery cells. If OCV curves are different, these differences can be associated to electrode stoichiometry dispersion in manufacturing. These dispersions can be assimilated to aging consequences and can be taken into account through an appropriated parameter $\alpha$.

This result is verified with the 4 cells battery pack. Table 1 shows that each $OCVC_{init}$ can be obtained by the mapping of each other cell. This table shows that a unique $OCVC_{init}$ can be used for the 4 cells (with a maximal error less than the measurement noise magnitude recorded when implemented in a car). The cell2 $OCVC_{init}$ is defined by (see relation (27)):

$$E_{init} = \sum_{k=0}^{N} D_k^{init} SOC^k \qquad (42)$$

with the following coefficients

| | | | | | |
|---|---|---|---|---|---|
| $D_0^{init}$ | 3.3477 | $D_1^{init}$ | 5.8209e-03 | $D_2^{init}$ | 1.51776e-05 |
| $D_3^{init}$ | 5.30509e-05 | $D_4^{init}$ | -4.84996e-06 | $D_5^{init}$ | 2.09160e-07 |
| $D_6^{init}$ | -7.39406e-09 | $D_7^{init}$ | 2.66133e-10 | $D_8^{init}$ | -7.73359e-12 |
| $D_9^{init}$ | 1.51006e-13 | $D_{10}^{init}$ | -1.87043e-15 | $D_{11}^{init}$ | 1.41031e-17 |
| $D_{12}^{init}$ | -5.90990e-20 | $D_{13}^{init}$ | 1.05615e-22 | | |

will be used in the following.

Table 1: $OCVC_{init}$ fitting of 4 cells using a unique polynomial and computation of parameter α. The grey boxes highlight the considered cell for polynomials fitting for each experience. The fitting maximal absolute errors are also gathered in the table for each experience.

| | $\alpha$ | | | | Maximal absolute error (mV) | | | |
|---|---|---|---|---|---|---|---|---|
| $OCVC_{init}$ | | | | | | | | |
| n° 1 | 1 | 0.98 | 0.96 | 1 | $4.10^{-2}$ | 7 | 9 | 8 |
| n° 2 | 1.02 | 1 | 0.99 | 1.02 | 8 | 2 | 12 | 12 |
| n° 3 | 1.03 | 1.01 | 1 | 1.04 | 23 | 11 | 3 | 5 |
| n° 4 | 1 | 0.98 | 0.97 | 1 | 17 | 11 | 4 | 2 |

## 3.3 OCV Curve Adjustment as Aging

The algorithm is based on the idea that for two OCV voltages $E_a$ and $E_b$ such that $E_a < E_b$, the state of charge variation $\Delta SOC(E_a, E_b)$ differs for each aging state, especially if voltage $E_a$ and $E_b$ are very different. This statement is demonstrated by expressing the state of charge variation $\Delta SOC(E_a, E_b)$ at the initial state and for two other aging states characterized by parameters $\alpha_I$ and $\alpha_{II}$. At initial state, state of charges leading to $OCV$ $E_a$ and $E_b$ are denoted $SOC_a^{init}$ and $SOC_b^{init}$ and are such that:

$$\Delta SOC(E_a; E_b)|_{init} = SOC_b^{init} - SOC_a^{init}$$
$$= \frac{\Delta Q(E_a; E_b)}{Q_{nom}} = -\frac{\int_{E=E_a}^{E=E_b} I}{Q_{nom}} \qquad (43)$$

Let then SOC denotes the state of charge of an aged cell and $SOC^{init}$ the state of charge of the same unused battery for the same OCV. According to relation (41), the two states of charge are linked by the relation:

$$SOC = \frac{1}{\alpha}\left(SOC^{init} - 1\right) + 1 \qquad (44)$$

At ageing state characterized by $\alpha_I$, state of charge variation between the two OCV $E_a$ and $E_b$ is

given by:

$$\Delta SOC(E_a; E_b)|_{\alpha_I} = \frac{1}{\alpha_I} \Delta SOC(E_a; E_b)|_{init} \qquad (45)$$

Similarly, at ageing state characterized by $\alpha_{II}$:

$$\Delta SOC(E_a; E_b)|_{\alpha_{II}} = \frac{1}{\alpha_{II}} \Delta SOC(E_a; E_b)|_{init} \qquad (46)$$

Aging difference characterized by $\alpha_I \neq \alpha_{II}$ implies a difference in state of charge variations:

$$\Delta SOC|_{\alpha_I} \neq \Delta SOC|_{\alpha_{II}} \qquad (47)$$

Thus, a measure $(\Delta SOC; E_a; E_b)$ corresponds to an unique OCV curve. With a set of $M \geq 2$ measures of state of charge variations $\Delta SOC(E_1; E_{t>1})$ with $E_1 < ... < E_M$, there will be $M - 1$ associated parameters $\alpha_t$.

If the measures are perfects, all parameters $\alpha_t$ are equals. If however measures are for instance marred by noise, an optimal parameter $\alpha$ allowing to accurately representing the experimental data must be deduced. To solve this problem, a least square problem can be formulated leading to the minimization of the following criterion:

$$J(\alpha) = \frac{1}{M-1} \sum_{t=2}^{M} \left( \begin{array}{c} \Delta SOC(E_1; E_t) \\ -\Delta SOC(E_1; E_t; \alpha) \end{array} \right)^2 \qquad (48)$$

## 3.4 Validation

The implementation of the OCV curve adjustment algorithm previously described requires at least two OCV measures. These measures are obtained here on voltage profiles presented in Figure 14.



Charge and measures (♦) used for OCV identification

Discharge for measure of validation points (♦)
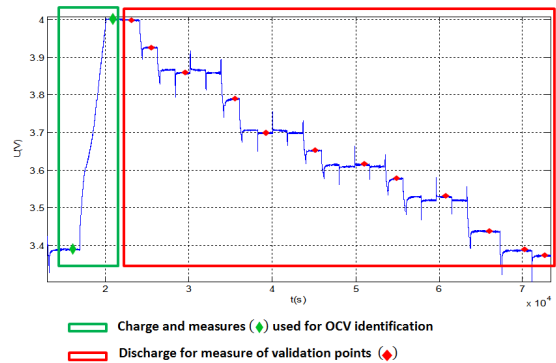
Figure 14: Example of charge profile providing two measures for OCV curve reconstruction (second measure at 4V) and OCV measure (during a discharge) for validation.

The charge part is used to get the two OCV measures required for the curve adjustment. The discharge part is used to get OCV measures required to validate the method. During discharge, the relaxation time after each step is about 30 minutes. On the discharge part the SOC information required for each validation points is calculated by current integration from the reference point for SOC = 100% defined by $E= E_{100\%}$ namely 4V.

Table 2 gives in column max($\varepsilon$) the 4 more important errors (on all measures of the discharge) and for 4 different temperatures. The column $\Delta E$ gives voltages variations due to aging. These errors are determined for the 6 aging denoted {A1, A2, A3, A4, A5, A6} that appears in figure 13.

Table 2: Maximum identification errors for different ageing and temperatures.

| Cell 2 | | $max(\varepsilon(mV))$ | | | | $\Delta E(mV)$ | | | |
|---|---|---|---|---|---|---|---|---|---|
| | | −10°C | 0°C | 20°C | 40°C | −10°C | 0°C | 20°C | 40°C |
| A2 | $\varepsilon_1$ | -9 | -15 | -23 | 19 | 22 | 53 | 42 | 27 |
| | $\varepsilon_2$ | -7 | -14 | -22 | 14 | 59 | 25 | 43 | 1 |
| | $\varepsilon_3$ | -6 | -9 | -18 | 12 | 63 | 49 | 22 | 3 |
| | $\varepsilon_4$ | -5 | -6 | -13 | 12 | 70 | 19 | 22 | 2 |
| A3 | $\varepsilon_1$ | | | 32 | | | | | 41 |
| | $\varepsilon_2$ | | | 23 | | | | | 36 |
| | $\varepsilon_3$ | | | -23 | | | | | 43 |
| | $\varepsilon_4$ | | | 14 | | | | | 49 |
| A4 | $\varepsilon_1$ | -33 | -36 | 42 | 37 | 133 | 97 | 35 | 139 |
| | $\varepsilon_2$ | -32 | -27 | 32 | 27 | 146 | 50 | 32 | 151 |
| | $\varepsilon_3$ | -28 | -15 | 29 | 16 | 151 | 159 | 151 | 76 |
| | $\varepsilon_4$ | -25 | -14 | -18 | -14 | 155 | 166 | 39 | 19 |
| A5 | $\varepsilon_1$ | -28 | -60 | 42 | 45 | 61 | 140 | 156 | 152 |
| | $\varepsilon_2$ | 16 | -47 | 35 | 36 | 62 | 231 | 109 | 106 |
| | $\varepsilon_3$ | 8 | -31 | 34 | 34 | 65 | 51 | 57 | 53 |
| | $\varepsilon_4$ | 8 | -29 | -18 | -16 | 78 | 211 | 41 | 62 |
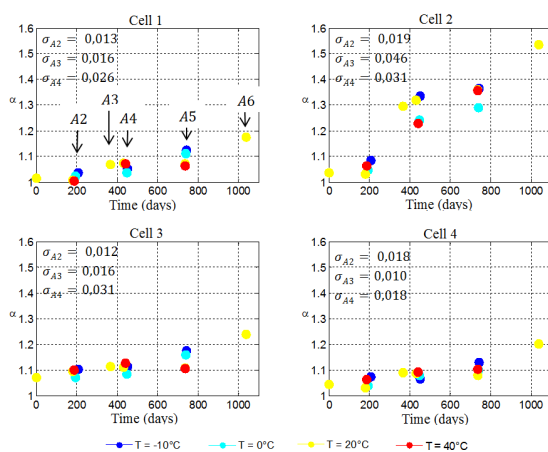


Figure 15: $\alpha$ variation according to aging for different temperatures.

Figure 15 shows parameter variations $\alpha$ according to temperature and cells aging. On this figure, $\alpha$ parameter value grows according to ageing. For cells 1, 3 and 4 the $\alpha$ values are more or less equals. For cell2 case, the ageing is more important and $\alpha$ is higher than 1.5 for measures at A6.

Figure 15 shows that OCV curves are very little affected by temperature, indeed no particular variations are noted on the parameter $\alpha$ when temperature is varying. The standard deviation, on $\alpha$ values, is higher for cell2 and on A4 measures ($\sigma_{A4}$). $\alpha$ variations are mainly attributed to identification errors.

## 4  CONCLUSIONS

The paper proposes a lithium-ion Open Circuit Voltage (OCV) curve model that requires only one parameter adjustment as batteries aging. Such a result has been obtained through an analysis of electrodes stoichiometries variations as ageing. A two steps algorithm is then proposed for model adjustment as aging. The first step is the identification of the OCV curve at initial state. In the second step, a parameter characterizing the aging of the cell is identified from at least two OCV measures in normal operation or in specific operation (charge phase for instance). The efficiency of this algorithm has been shown with a battery pack constituted of four Lithium-ion cells. The modelling error remains small in spite of cells aging and temperature variations. Moreover, the OCV curve adjustment as cell aging requires the optimization of only one parameter and this parameter variations can be correlated to battery aging. This parameter can thus be viewed as a State Of Health (SOH) indicator.

The authors have recently proposed lithium-ion cells models based on fractional differentiation (Sabatier et al, 2014). They now intend to include the OCV curve adjustment method proposed in this paper into the cell model and also to propose adjustment methods for the other model parameter in order to get a cell model that is robust versus aging.

# REFERENCES

Armand M., Tarascon J. M., Building better batteries, *Nature* 451, pp 652-657, 2008.

Arora, P, White R. E., Doyle M. Capacity Fade Mechanisms and Side Reactions in Lithium-Ion Batteries, *Journal of the Electrochemical Society,* Vol. 145, N° 10, pp. 3647–67.

Bard A. J., Inzelt G., Scholz F., *Electrochemical Dictionary* Springer-Verlag Berlin Heidelberg. 2008.

Cheng M. W., Lee Y. S., Liu M., Sun C. C., State-of-charge estimation with aging effect and correction for lithium-ion battery, *Electrical Systems in Transportation, IET,* Vol. 5, N° 2, 2015.

Dubarry M., Liaw B.Y., Identify capacity fading mechanism in a commercial LiFePO4 cell, J. *Power Sources* 194, pp 541-549, 2009.

Francisco J. M., Sabatier J., Lavigne L., Guillemard F., Moze M., Tari M., Merveillaut M., Noury A., Lithium-ion battery state of charge estimation using a fractional battery model, *IEEE International Conference on Fractional Differentiation and its Applications*, 23-25 June 2014, Catania, Italy.

Honkuraa K., Honboa H., Koishikawab Y., Horibab T., State Analysis of Lithium-Ion Batteries Using Discharge Curves, *ECS Transaction*, Vol. 13, pp 61-73, 2008.

Hu Y., Yurkovich S., Guezennec Y., Yurkovich B., Electro-thermal battery model identification for automotive applications, *J. Power Sources* 196, pp 449-457, 2011.

Karthikeyan D. K, Sikha G, White R. E., Thermodynamic Model Development for Lithium Intercalation Electrodes, *J. Power Sources*, 185: pp1398–1407. 2008.

Kim I. S., A Technique for Estimating the State of Health of Lithium Batteries Through a Dual-Sliding-Mode Observer, *IEEE Transactions on power electronics*, Vol. 25, No. 4, April 2010.

Liaw B. Y., Dubarry M., in: G. Pistoia (Ed.), *Electric and Hybrid Vehicles: Power Sources, Models, Sustainability, Infrastructure and the Market*, Elsevier, pp. 375-403, 2010.

Lee S., Kim J., Lee J., Cho B. H., State-of-charge and capacity estimation of lithium-ion battery using a new open-circuit voltage versus state-of-charge, *Journal of Power Sources*, vol. 185, no. 2, pp. 1367–1373, 2008.

Petzl M., Danzer, M. A., Advancements in OCV Measurement and Analysis for Lithium-Ion Batteries. *IEEE Transactions on Energy Conversion*, 28(3), pp.675–681., 2013.

Piller S., Perrin M., Jossen A., Methods for state-of-charge determination and their applications, *Journal of Power Sources* 96 (2001) 113-120, 2001.

Plett G. L., Extended Kalman filtering for battery management systems of LiPB-based HEV battery packs Part 3. State and parameter estimation, *Journal of Power Sources*, 134, 277–292, 2004.

Pop V., Bergveldb H. J., Regtiena P. P. L., Op het Veldc J. H. G., Danilovd D., Notten P. H. L., Battery Aging and Its Influence on the Electromotive Force. *Journal of The Electrochemical Society*, 154(8), p.A744-A750, 2007.

Roscher M.A., Assfalg J., Bohlen O.S., Detection of Utilizable Capacity Deterioration in Battery Systems, *IEEE Trans. Veh. Technol*. 60 pp. 98-103, 2011.

Roscher, M.A., Bohlen, O., Vetter, J., OCV Hysteresis in Li-Ion Batteries including Two-Phase Transition Materials, *International Journal of Electrochemistry*, pp.1–6,2011.

Sabatier J., Merveillaut M., Francisco J., Guillemard F., Lithium-ion batteries modelling involving fractional differentiation, *Journal of power sources*, 262C, pp. 36-43, 2014.

Sabatier J., Francisco J., Guillemard F., Lavigne L., Moze M., Merveillaut M., Lithium-ion batteries modelling: a simple fractional differentiation based model and its associated parameters estimation method, *Signal Processing*, Vol 207, pp. 290-301, 2015.

Santhanagopalan S., White R. E., Online estimation of the state of charge of a lithium ion cell, *Journal of Power Sources* 161, pp 1346-1355, 2006.

Schmidt, J.P., Tran H. Y., Richtera J., Ivers-Tifféea E., Wohlfahrt-Mehrensb M., Analysis and prediction of the open circuit potential of lithium-ion cells. *Journal of Power Sources*, 239, pp.696–704, 2013.

Weng C, Sun J., Peng H., A unified open-circuit-voltage model of lithium-ion batteries for state-of-charge estimation and state-of-health monitoring, *Journal of Power Sources*, vol. 258, pp. 228-237, 2014.